Available online at www.sciencedirect.com
SCIENCE DIRECT®
Ecological Modelling 187 (2005) 369–388
ECOLOGICAL MODELLING
www.elsevier.com/locate/ecolmodel

An inverse ecosystem model of year-to-year variations with first order approximation to the annual mean fluxes

Zhenwen Wan [a,b,*], Joe Vallino [a]

[a] *The Ecosystems Center, Marine Biological Laboratory, Woods Hole, MA 02543, USA*
[b] *Key Laboratory of Marine Environmental Science, Xiamen University, Ministry of Education, Xiamen 361005, China*

Received 5 August 2003; received in revised form 28 January 2005; accepted 17 February 2005
Available online 19 March 2005

Abstract

Ecosystems exhibit nonlinear dynamics that are often difficult to capture in models. Consequently, linearization is commonly applied to remove some of the uncertainties associated with the nonlinear terms. However, since the true model is unknown and the operating point to linearize the model about is uncertain, developing linear ecosystems models is non-trivial. To develop a linear ecosystem model, we assume that the annual mean state of an ecosystem is a minor bias from the long-term mean state. A first order approximation inverse model to govern the year-to-year dynamics of ecosystems whose characteristic time scales are less than 1 year is developed, through theoretically formulation, on the basis of steady state analysis, time scale separation and nondimensionalization. The approach is adept at predicting year-to-year variations and to tracking system response to changes in environmental drivers when compared to data generated with a standard nonlinear *NPZD* model.

Keywords: Inverse model; Ecosystem modeling; First order approximation; Flux analysis; Time scale separation

1. Introduction

One of the primary goals of ecology is to understand the response of an ecosystem to changes in environmental drivers. The realization of this goal is that one can predict the ecosystem's variation to environmental drivers once an appropriate model has been developed. The basis of model development is mathematically approximating the instantaneous and/or short-term response of the organism to its environment. For example, the temperature–photosynthesis relationship, $Q_{10}^{(T-10)/10}$ (Eppley, 1972), the light–photosynthesis relationship, $(I/I_o)\exp(1-(I/I_o))$ (Steel, 1962), the Michaelis–Menten function, $N/(N+K)$, are all instantaneous functions with respect to environmental variables of temperature T, light intensity I, and limiting nutrient concentration N, respectively. However, the practical concern in environmental ecology is often the year-to-year variations and/or long-term variations rather than short-term ones. For example, annual yield in fishery ecology is the scale of interest, not instantaneous or daily yield.

* Corresponding author. Tel.: +86 592 218 2811; fax: +86 592 218 0655.
E-mail address: zwan@xmu.edu.cn (Z. Wan).

0304-3800/$ – see front matter © 2005 Elsevier B.V. All rights reserved.
doi:10.1016/j.ecolmodel.2005.02.003

There are two major challenges to develop a model based on the rules governing the instantaneous biology-environment interactions. First, one needs to supply information that describes the short-term changes in environmental drivers; however, it is difficult to obtain accurate predictions on the dynamics of environmental drivers very far into the future, which is necessary for daily/seasonal ecological model simulations. Generally, long-term trends are less difficult to obtain, such as annual average temperature 50 years into the future. Second, short-term tends are more difficult to understand and explain than long-term trends. Consider fishery yield. A daily yield hardly makes sense. Daily variation has a far larger range than that of the annual mean daily yield. Models used to describe short-term dynamics require more state variables and more parameters for each state equation than models used to describe annual mean variations.

If instead, the modeling focus is placed on long-term trends, then the above two challenges can be mitigated. However, the rules that govern the long-term mean response cannot be derived from the rules that govern short-term dynamics. For instance, it has been shown that calculating long-term expected values of temperature dependent functions can seldom be achieved by applying the functions to mean temperature (Lischke et al., 1997), because temperature dependencies are often nonlinear. Short-term rules are developed through short-term experiments and/or observations. It is possible to do the same for long-term rules provided long-term experiments and/or observations are available. If data are available, inverse methods can be used to estimate flows between compartments (Vézina and Platt, 1988); however, flow analysis models cannot be used for prediction. Although standard state space models can be used for prediction, almost all of the models developed thus far focus on short-term dynamics and are not applicable to long-term behavior. The main contribution of this manuscript is to combine flow analysis with first order approximations of process rates to predict ecosystem annual dynamics. Consequently, our approach allows the long-term response of an ecosystem to be predictable from the long-term mean environmental drivers.

In brief, steady state analysis, linearization, time scale separation, and dimensional analysis are employed to formulate a first order approximation model to describe the year-to-year dynamics of an ecosystem in which nutrient and organismal concentrations are annual averaged. An inverse method is used to estimate model parameters. A typical *NPZD* compartment model is used to generate simulated observations and test the first order approximation model. A forecast experiment is carried out to test the predictive capability of this model.

2. Model formulation

2.1. A steady state analysis

Although steady state analysis applied to ecosystems has an extensive and controversial history (Nilsson and Grelsson, 1995), the qualitative concepts will be useful for our model development and should not be interpreted in a strict mathematical sense. A mature ecosystem can be thought of as being in a steady state or, if inherently chaotic, in low amplitude oscillations about an attractor. This steady state allows for diel and annual fluctuations, but the ecosystem's description necessarily takes place at some averaged level. Given a permanent alteration of the ecosystem drivers, it will settle on a new steady state, again in some spatially and temporally averaged sense (van den Berg, 1998). What do we consider a mature ecosystem? What alterations may be considered as permanent? We tentatively assume that an ecosystem remains at steady state, once the environmental drivers are constant with respect to a given temporal scale. When the surroundings change to a new value, the ecosystem will transfer to a new steady state after a certain transient time. The transient time required to reach a new steady state is on the order of the doubling time of the slowest growing organism. For example, in a planktonic ecosystem, the response time is less than 1 month.

For model development purposes, we will consider a plankton ecosystem composed of four compartments: nutrient N, phytoplankton P, zooplankton Z and detritus D with mass flow connectivity as illustrated in Fig. 1. We assume that under the long-term averaged surroundings of temperature T and light L, this system attains a steady state (SS) with stocks $\underline{\underline{N}}$, $\underline{\underline{P}}$, $\underline{\underline{Z}}$, $\underline{\underline{D}}$, and fluxes $\underline{\underline{f}}_1$, $\underline{\underline{f}}_2$, $\underline{\underline{f}}_3$, $\underline{\underline{f}}_4$ and $\underline{\underline{f}}_5$. According to the mass flow connectivity (Fig. 1), the following conservation

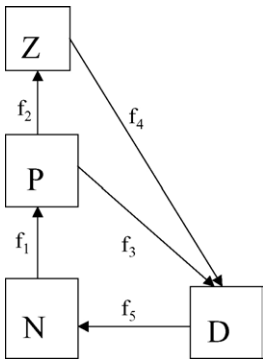

Fig. 1. Food web of a typical marine plankton ecosystem model. *N*, *P*, *Z*, and *D* stand for concentrations of dissolve inorganic nutrient, phytoplankton, zooplankton and detritus, respectively.

equations exist under SS conditions,

$$\begin{aligned}
&\bar{\bar{f}}_5 - \bar{\bar{f}}_1 = 0\\
&\bar{\bar{f}}_1 - \bar{\bar{f}}_2 - \bar{\bar{f}}_3 = 0\\
&\bar{\bar{f}}_2 - \bar{\bar{f}}_4 = 0\\
&\bar{\bar{f}}_3 + \bar{\bar{f}}_4 - \bar{\bar{f}}_5 = 0.
\end{aligned} \tag{1}$$

Once the surroundings change to a new state with temperature $\bar{T}$ and light $\bar{L}$, the system reaches a new SS with stocks $\bar{N}$, $\bar{P}$, $\bar{Z}$ and $\bar{D}$ and fluxes $\bar{f}_1$, $\bar{f}_2$, $\bar{f}_3$, $\bar{f}_4$ and $\bar{f}_5$. During the transient period $\Delta\theta$, this system may be approximated with fixed fluxes $\hat{f}_1$, $\hat{f}_2$, $\hat{f}_3$, $\hat{f}_4$ and $\hat{f}_5$ and constant state change,

$$\begin{aligned}
&\hat{f}_5 - \hat{f}_1 = \frac{\bar{N} - \bar{\bar{N}}}{\Delta\theta}\\
&\hat{f}_1 - \hat{f}_2 - \hat{f}_3 = \frac{\bar{P} - \bar{\bar{P}}}{\Delta\theta}\\
&\hat{f}_2 - \hat{f}_4 = \frac{\bar{Z} - \bar{\bar{Z}}}{\Delta\theta}\\
&\hat{f}_3 + \hat{f}_4 - \hat{f}_5 = \frac{\bar{D} - \bar{\bar{D}}}{\Delta\theta}.
\end{aligned} \tag{2}$$

We now place the above example in general form. Define $\boldsymbol{x}$ as the ecosystem state vector, $\boldsymbol{e}$ the environmental driver vector, $\boldsymbol{f}$ the flux vector and $\boldsymbol{A}$ as the matrix which represents the food web connectivity. The dynamics of this ecosystem can then be expressed as,

$$\frac{\mathrm{d}\boldsymbol{x}}{\mathrm{d}\theta} = \boldsymbol{A}\boldsymbol{f}(\boldsymbol{x}, \boldsymbol{e}) \tag{3}$$

where θ is the time, and $\boldsymbol{f}$ depends on $\boldsymbol{x}$ and $\boldsymbol{e}$. With respect to the first SS, the environmental driver is $\bar{\bar{\boldsymbol{e}}}$, the stock is $\bar{\bar{\boldsymbol{x}}}$ and the flux is $\bar{\bar{\boldsymbol{f}}}$, so Eq. (1) can be written as,

$$\boldsymbol{A}\bar{\bar{\boldsymbol{f}}} = 0. \tag{4}$$

We assign definitions of $\bar{\boldsymbol{x}}$, $\bar{\boldsymbol{e}}$ and $\bar{\boldsymbol{f}}$ for the second SS similar to $\bar{\bar{\boldsymbol{x}}}$, $\bar{\bar{\boldsymbol{e}}}$ and $\bar{\bar{\boldsymbol{f}}}$ for the first SS. The approximation of the system dynamics during the transient period between two steady states may be expressed as,

$$\boldsymbol{A}\hat{\boldsymbol{f}} = \frac{\bar{\boldsymbol{x}} - \bar{\bar{\boldsymbol{x}}}}{\Delta\theta} \tag{5}$$

where $\hat{\boldsymbol{f}}$ stands for the average flux vector during the transient period.

Linearization is a common mathematical approach. However, choosing the appropriate operating point to linearize around can be challenging, since the linear model approximates the true system only in the neighborhood of the chosen operating point. Linearization is uncommon in ecological modeling, although there are applications in flow estimation and sensitivity analysis (Kooi et al., 2002; Köhler and Wirtz, 2002; Diffendorfer et al., 2001; van den Berg, 1998). A SS may be an ideal operating point for linearization about. Thus, a Taylor expansion of $\hat{\boldsymbol{f}}$ about $\bar{\bar{\boldsymbol{x}}}$ and $\bar{\bar{\boldsymbol{e}}}$, evaluated at $\bar{\boldsymbol{x}}$ and $\bar{\boldsymbol{e}}$, keeping only the first order terms, gives an approximation for $\hat{\boldsymbol{f}}$,

$$\hat{\boldsymbol{f}} \cong \bar{\bar{\boldsymbol{f}}} + \left.\frac{\partial \boldsymbol{f}}{\partial \boldsymbol{x}}\right|_{\bar{\bar{\boldsymbol{x}}},\bar{\bar{\boldsymbol{e}}}} (\bar{\boldsymbol{x}} - \bar{\bar{\boldsymbol{x}}}) + \left.\frac{\partial \boldsymbol{f}}{\partial \boldsymbol{e}}\right|_{\bar{\bar{\boldsymbol{x}}},\bar{\bar{\boldsymbol{e}}}} (\bar{\boldsymbol{e}} - \bar{\bar{\boldsymbol{e}}}) \tag{6}$$

For simplicity, we define matrixes $\boldsymbol{G}_1$ and $\boldsymbol{G}_2$ in the following expression,

$$\begin{aligned}
\boldsymbol{G}_1 &= \left.\frac{\partial \boldsymbol{f}}{\partial \boldsymbol{x}}\right|_{\bar{\bar{\boldsymbol{x}}},\bar{\bar{\boldsymbol{e}}}}\\
\boldsymbol{G}_2 &= \left.\frac{\partial \boldsymbol{f}}{\partial \boldsymbol{e}}\right|_{\bar{\bar{\boldsymbol{x}}},\bar{\bar{\boldsymbol{e}}}}.
\end{aligned} \tag{7}$$

Therefore, Eq. (5), with application of Eq. (4), can be rewritten as,

$$\boldsymbol{A}(\boldsymbol{G}_1(\bar{\boldsymbol{x}} - \bar{\bar{\boldsymbol{x}}}) + \boldsymbol{G}_2(\bar{\boldsymbol{e}} - \bar{\bar{\boldsymbol{e}}})) \cong \frac{\bar{\boldsymbol{x}} - \bar{\bar{\boldsymbol{x}}}}{\Delta\theta}. \tag{8}$$

Eq. (8) is a first order approximation model derived from a steady state analysis combined with linearization, but the representation of time scale is unclear. Since Eq. (5) represents the transient response, the validity of the linearization, Eq. (6), is time scale dependent. It may literally represent an evenly transforming process from one steady state to another, but may not

be applicable to all SS transitions. The following time scale analysis will explain the meaning of the evenly transforming process from the long-term mean state to the annual mean state.

2.2. Time scale separation

Choice of the appropriate time scale is also an import consideration for model development. Time scale separation is quite common in geophysics. For example, hydrodynamic time scales are classified as circulation, tidal current and turbulent current in oceanography. Time scale concepts have been recognized in ecology recently. Although different time scales were assumed in the trophic levels by Kooi et al. (1998), no complete time scale separation was carried out. Similarly, different methods were used for hourly, daily, and monthly temperatures to describe the temperature dependency of an ecosystem (Lischke et al., 1997). We associate the primary SS with a long-term mean state of a pristine ecosystem and the secondary SS with the annual mean state. We formulate the first order approximation model through time scale separation in the following context.

We define the long-term mean values of $\boldsymbol{x}$, $\boldsymbol{e}$, and $\boldsymbol{f}$, which are time dependent as,

$$\begin{aligned}\bar{\bar{\boldsymbol{x}}} &= \int_{-\infty}^{+\infty} \boldsymbol{x}(\theta)\,\mathrm{d}\theta \\ \bar{\bar{\boldsymbol{e}}} &= \int_{-\infty}^{+\infty} \boldsymbol{e}(\theta)\,\mathrm{d}\theta \\ \bar{\bar{\boldsymbol{f}}} &= \int_{-\infty}^{+\infty} \boldsymbol{f}(\theta)\,\mathrm{d}\theta\end{aligned} \quad . \tag{9}$$

We express time θ by two scales,

$$\theta = n\Delta\theta + \delta\theta, \tag{10}$$

where n stands for year number, $\Delta\theta$ for 1 year and $\delta\theta$ for seasonal time, whose maximum increment is less than $\Delta\theta$. We define annual mean values,

$$\begin{aligned}\bar{\boldsymbol{x}}(n\Delta\theta) &= \int_{-\Delta\theta/2}^{+\Delta\theta/2} \boldsymbol{x}(n\Delta\theta+\delta\theta)\,\mathrm{d}\delta\theta \\ \bar{\boldsymbol{e}}(n\Delta\theta) &= \int_{-\Delta\theta/2}^{+\Delta\theta/2} \boldsymbol{e}(n\Delta\theta+\delta\theta)\,\mathrm{d}\delta\theta \\ \bar{\boldsymbol{f}}(n\Delta\theta) &= \int_{-\Delta\theta/2}^{+\Delta\theta/2} \boldsymbol{f}(n\Delta\theta+\delta\theta)\,\mathrm{d}\delta\theta\end{aligned} \tag{11}$$

the seasonal variations,

$$\begin{aligned}\boldsymbol{x}''(n\Delta\theta,\delta t) &= \boldsymbol{x}(\theta) - \bar{\boldsymbol{x}}(n\Delta\theta) \\ \boldsymbol{e}''(n\Delta\theta,\delta t) &= \boldsymbol{e}(\theta) - \bar{\boldsymbol{e}}(n\Delta\theta) \\ \boldsymbol{f}''(n\Delta\theta,\delta t) &= \boldsymbol{f}(\theta) - \bar{\boldsymbol{f}}(n\Delta\theta),\end{aligned} \tag{12}$$

and the annual mean biases from the long-term mean,

$$\begin{aligned}\boldsymbol{x}'(n\Delta\theta) &= \bar{\boldsymbol{x}}(n\Delta\theta) - \bar{\bar{\boldsymbol{x}}} \\ \boldsymbol{e}'(n\Delta\theta) &= \bar{\boldsymbol{e}}(n\Delta\theta) - \bar{\bar{\boldsymbol{e}}} \\ \boldsymbol{f}'(n\Delta\theta) &= \bar{\boldsymbol{f}}(n\Delta\theta) - \bar{\bar{\boldsymbol{f}}}.\end{aligned} \tag{13}$$

According to the above definitions, $\boldsymbol{x}(\theta)$, $\boldsymbol{e}(\theta)$, and $\boldsymbol{f}(\theta)$ can be expressed as,

$$\begin{aligned}\boldsymbol{x}(\theta) &= \bar{\bar{\boldsymbol{x}}} + \boldsymbol{x}'(n\Delta\theta) + \boldsymbol{x}''(n\Delta\theta,\delta\theta) \\ \boldsymbol{e}(\theta) &= \bar{\bar{\boldsymbol{e}}} + \boldsymbol{e}'(n\Delta\theta) + \boldsymbol{e}''(n\Delta\theta,\delta\theta) \\ \boldsymbol{f}(\theta) &= \bar{\bar{\boldsymbol{f}}} + \boldsymbol{f}'(n\Delta\theta) + \boldsymbol{f}''(n\Delta\theta,\delta\theta)\end{aligned} \quad . \tag{14}$$

We approximate the flux function $\boldsymbol{f}(\theta) = \boldsymbol{f}(\boldsymbol{x},\boldsymbol{e})$ about an arbitrary point, $(\boldsymbol{x}_0,\boldsymbol{e}_0)$, keeping only the first order terms,

$$\begin{aligned}\boldsymbol{f}(\theta) &= \boldsymbol{f}(\boldsymbol{x},\boldsymbol{e}) \\ &\cong \boldsymbol{f}_0 + \left.\frac{\partial \boldsymbol{f}}{\partial \boldsymbol{x}}\right|_{\boldsymbol{x}_0,\boldsymbol{e}_0} (\boldsymbol{x}-\boldsymbol{x}_0) + \left.\frac{\partial \boldsymbol{f}}{\partial \boldsymbol{e}}\right|_{\boldsymbol{x}_0,\boldsymbol{e}_0} (\boldsymbol{e}-\boldsymbol{e}_0).\end{aligned} \tag{15}$$

We use the time scale representations of $\boldsymbol{x}$ and $\boldsymbol{e}$, Eq. (14), to get,

$$\begin{aligned}\boldsymbol{f}(\theta) &= \boldsymbol{f}(\boldsymbol{x},\boldsymbol{e}) \\ &\cong \boldsymbol{f}_0 + \left.\frac{\partial \boldsymbol{f}}{\partial \boldsymbol{x}}\right|_{\boldsymbol{x}_0,\boldsymbol{e}_0} (\bar{\bar{\boldsymbol{x}}} + \boldsymbol{x}'(n\Delta\theta) + \boldsymbol{x}''(n\Delta\theta,\delta\theta) - \boldsymbol{x}_0) \\ &\quad + \left.\frac{\partial \boldsymbol{f}}{\partial \boldsymbol{e}}\right|_{\boldsymbol{x}_0,\boldsymbol{e}_0} (\bar{\bar{\boldsymbol{e}}} + \boldsymbol{e}'(n\Delta\theta) + \boldsymbol{e}''(n\Delta\theta,\delta\theta) - \boldsymbol{e}_0).\end{aligned} \tag{16}$$

Once we separate $\boldsymbol{f}(\theta)$ into its time scale representation, Eq. (14), we have,

$$\begin{aligned}f'(n\Delta\theta) &= \boldsymbol{G}_1\boldsymbol{x}'(n\Delta\theta) + \boldsymbol{G}_2\boldsymbol{e}'(n\Delta\theta) \\ f''(n\Delta\theta,\delta\theta) &= \boldsymbol{G}_1\boldsymbol{x}''(n\Delta\theta,\delta\theta) + \boldsymbol{G}_2\boldsymbol{e}''(n\Delta\theta,\delta\theta).\end{aligned} \tag{17}$$

When we integrate Eq. (3) from time θ_0 to time θ, assuming $\theta - \theta_0 = \Delta\theta$, using the time separated variables (Eq. (14)), we obtain,

$$\begin{aligned}&\bar{\bar{\boldsymbol{x}}} + \boldsymbol{x}'(n\Delta\theta) + \boldsymbol{x}''(n\Delta\theta,\delta\theta) \\ &\quad = \boldsymbol{x}(\theta_0) + \int_{\theta_0}^{\theta} \boldsymbol{A}\left(\bar{\bar{\boldsymbol{f}}} + \boldsymbol{f}'(n\Delta\theta) + \boldsymbol{f}''(n\Delta\theta,\delta\theta)\right) \\ &\qquad \times \mathrm{d}\delta\theta\end{aligned} \tag{18}$$

Since the initial conditions, $\boldsymbol{x}(\theta_0)$, are typically not well known and their influence on the current state rapidly decays with time, we can set $\boldsymbol{x}(\theta_0)$ equal to the long-term mean, $\bar{\bar{\boldsymbol{x}}}$, with little loss of generality. Thus, we can transform Eq. (18) into the following form,

$$\boldsymbol{x}'(n\Delta\theta) + \boldsymbol{x}''(n\Delta\theta, \delta\theta) = \Delta\theta \boldsymbol{A}\bar{\bar{\boldsymbol{f}}} + \Delta\theta \boldsymbol{A}\boldsymbol{f}'(n\Delta\theta) + \int_{\delta\theta-\Delta\theta}^{\delta\theta} \boldsymbol{A}\boldsymbol{f}''(n\Delta\theta, \delta\theta) \times \mathrm{d}\delta\theta. \quad (19)$$

We separate the time scales, which gives us the following two equations,

$$\boldsymbol{x}''(n\Delta\theta, \delta\theta) = \int_{\delta\theta-\Delta\theta}^{\delta\theta} \boldsymbol{A}\boldsymbol{f}''(n\Delta\theta, \delta\theta)\,\mathrm{d}\delta\theta \quad (20)$$

$$\boldsymbol{x}'(n\Delta\theta) = \Delta\theta \boldsymbol{A}\bar{\bar{\boldsymbol{f}}} + \Delta\theta \boldsymbol{A}\boldsymbol{f}'(n\Delta\theta). \quad (21)$$

With substitution of Eqs. (4) and (17) into Eq. (21), we obtain,

$$\boldsymbol{x}'(n\Delta\theta) = \Delta\theta \boldsymbol{A}\boldsymbol{f}'(n\Delta\theta) = \Delta\theta \boldsymbol{A}(\boldsymbol{G}_1\boldsymbol{x}'(n\Delta\theta) + \boldsymbol{G}_2\boldsymbol{e}'(n\Delta\theta)). \quad (22)$$

Eq. (22) is similar to Eq. (8), but is specific for the annual mean bias from the long-term mean, which is the time scale of interest.

2.3. Dimensional analysis

Dimensional analysis transforms the variables in a problem to a reduced set of dimensionless variables. This transformation helps to reveal the nature of relationships among variables, simplifies modeling, and produces predictions that are readily compared across species and conditions (Stephen and Dunbar, 1993). Although most ecosystem models are not based on dimensionless variables, the convenience of dimensionless parameters has been increasingly recognized (Ebert et al., 2001; Wan et al., 2000a; van den Berg, 1998). The application of dimensionless variables is not only convenient to generalize the representation of model parameters, but can also reduce the number of model parameters. We introduce the notation $[\cdot]$ to stand for the dimension of a variable or an expression. The basic ecosystem dimensions are $[\theta]$, $[\boldsymbol{x}]$, and $[\boldsymbol{e}]$ for θ, $\boldsymbol{x}$ and $\boldsymbol{e}$, respectively. Although $\boldsymbol{G}_1$, and $\boldsymbol{G}_2$ are defined by Eq. (7), we can consider them as unknown model parameters that have the following units,

$$[\boldsymbol{G}_1] = [\theta]^{-1}, \quad [\boldsymbol{G}_2] = [\theta]^{-1}[\boldsymbol{x}][\boldsymbol{e}]^{-1}. \quad (23)$$

Dimensionless coefficients have wide generality and enable cross-site use (Stephen and Dunbar, 1993). Using $\Delta\theta$, $\bar{\bar{\boldsymbol{x}}}$, and $\bar{\bar{\boldsymbol{e}}}$ as critical variables with dimensions $[\theta]$, $[\boldsymbol{x}]$, and $[\mathbf{e}]$, we can replace the model parameters $\boldsymbol{G}_1$, $\boldsymbol{G}_2$ with dimensionless coefficients $\boldsymbol{C}_1$, $\boldsymbol{C}_2$,

$$\boldsymbol{C}_1 = \boldsymbol{G}_1\Delta\theta, \quad \boldsymbol{C}_2 = \boldsymbol{G}_2\Delta\theta\bar{\bar{\boldsymbol{x}}}^{-1}\bar{\bar{\boldsymbol{e}}}. \quad (24)$$

2.4. The first order approximation inverse model

With substitution of Eq. (24) into Eq. (22) we obtain,

$$\boldsymbol{x}'(n\Delta\theta) = \Delta\theta \boldsymbol{A}\boldsymbol{f}'(n\Delta\theta) = \boldsymbol{A}\left(\boldsymbol{C}_1\boldsymbol{x}'(n\Delta\theta) + \boldsymbol{C}_2\frac{\bar{\bar{\boldsymbol{x}}}}{\bar{\bar{\boldsymbol{e}}}}\boldsymbol{e}'(n\Delta\theta)\right), \quad (25)$$

which is the first order approximation model for year-to-year dynamics, and forms the basis for all subsequent development. Since one can introduce different critical variables, this model may have different forms of rescaled dimensionless variables. This model equation is linear, but implicit. The model parameters $\boldsymbol{C}_1$, and $\boldsymbol{C}_2$ do not have direct biological meanings, but reflect the influence of $\boldsymbol{x}$ and $\boldsymbol{e}$ on $\boldsymbol{f}'$. Consequently, the parameters cannot be derived from first principles, but can be determined by inverse methods in a whole ecosystem context.

3. Application of approximation model to marine foodweb

Here we demonstrate application of the first-order approximation model (Eq. (25)) to a marine ecosystem. However, to facilitate analysis of our approach, data will be generated using a standard nonlinear *NPZD* model instead of actual observations.

3.1. NPZD model

We use a standard marine plankton model (Fig. 1) to generate simulated observations that are governed by the following differential equations (Wan et al., 2000b),

$$\begin{aligned}
\frac{\mathrm{d}P}{\mathrm{d}t} &= q_{10p}2^{0.1T-1.0}\frac{I}{I_o}\exp\left(1-\frac{I}{I_o}\right)\frac{N}{N+K_N}P \\
&\quad -m_P P - q_{10z}2^{0.1T-1.0}\frac{P}{P+K_P}Z \\
\frac{\mathrm{d}Z}{\mathrm{d}t} &= \beta q_{10z}2^{0.1T-1.0}\frac{P}{P+K_P}Z - m_Z Z \\
\frac{\mathrm{d}N}{\mathrm{d}t} &= -q_{10p}2^{0.1T-1.0}\frac{I}{I_o}\exp\left(1-\frac{I}{I_o}\right) \\
&\quad \times \frac{N}{N+K_N}P + \gamma D \frac{\mathrm{d}D}{\mathrm{d}t} = m_P P + m_Z Z \\
&\quad +(1-\beta)q_{10z}2^{0.1T-1.0}\frac{P}{P+K_P}Z - \gamma D
\end{aligned} \tag{26}$$

where P, Z, N, D, T, and I stand for phytoplankton, zooplankton, nutrients, detritus, water temperature and solar intensity, respectively. The model parameters are described in Table 1.

In this simplified model, phytoplankton respiration is accounted for by reducing their specific growth rate. Both mortality rates of phytoplankton and zooplankton are assumed proportional to compartment concentration. A fixed fraction of total zooplankton consumption is allocated to growth while the rest contributes to detritus production. A constant detritus decomposition rate is used.

3.2. A first order approximation model for the NPZD ecosystem

Eq. (25) is used to approximate the flux expressions. There are five fluxes in the simulated food web (Fig. 1), which are given by,

$$\begin{aligned}
f_1 &= q_{10p}2^{0.1T-1.0}\frac{I}{I_o}\exp\left(1-\frac{I}{I_o}\right)\frac{N}{N+K_N}P \\
f_2 &= q_{10z}2^{0.1T-1.0}\frac{P}{P+K_P}Z \\
f_3 &= m_P P \\
f_4 &= (1-\beta)q_{10z}2^{0.1T-1.0}\frac{P}{P+K_P}Z + m_Z Z \\
f_5 &= \gamma D
\end{aligned} \tag{27}$$

According to Eqs. (25) and (27), the first order approximation of year-to-year flux variations may be written as,

$$\begin{aligned}
f_1' &= c_{11}N' + c_{12}P' + c_{15}\frac{\bar{\bar{N}}}{\bar{\bar{T}}}T' + c_{16}\frac{\bar{\bar{N}}}{\bar{\bar{T}}}I' \\
f_2' &= c_{22}P' + c_{23}Z' + c_{25}\frac{\bar{\bar{P}}}{\bar{\bar{T}}}T' \\
f_3' &= c_{32}P' \\
f_4' &= c_{42}P' + c_{43}Z' + c_{45}\frac{\bar{\bar{Z}}}{\bar{\bar{T}}}T' \\
f_5' &= c_{54}D'
\end{aligned} \quad . \tag{28}$$

where C_{11}, C_{12}, C_{15}, C_{16}, C_{22}, C_{23}, C_{25}, C_{32}, C_{42}, C_{43}, C_{45}, and C_{54} are the coefficients of the first order approximation to the fluxes. Note that the symbol $\boldsymbol{x}'$ stands for the annual mean bias of $\boldsymbol{x}$ from its long-term mean, as before, and that $\boldsymbol{x}'$ is actually a function of $n\Delta\theta$; however, we drop the dependency $(n\Delta\theta)$ for simplicity hereafter. We note here that Eq. (28) is typically constructed from knowledge about the ecosystem under study, and not from a preexisting model, as in this example. Substituting Eq. (28) into Eq. (25) and noting $\Delta\theta = 1$ year, the first order approximation model for the NPZD marine ecosystem becomes,

$$\begin{pmatrix} N' \\ P' \\ Z' \\ D' \end{pmatrix} = \begin{pmatrix} -1 & 0 & 0 & 0 & 1 \\ 1 & -1 & -1 & 0 & 0 \\ 0 & 1 & 0 & -1 & 0 \\ 0 & 0 & 1 & 1 & -1 \end{pmatrix} \times \begin{pmatrix} c_{11}N' + c_{12}P' + c_{15}\dfrac{\bar{\bar{N}}}{\bar{\bar{T}}}T' + c_{16}\dfrac{\bar{\bar{N}}}{\bar{\bar{I}}}I' \\ c_{22}P' + c_{23}Z' + c_{25}\dfrac{\bar{\bar{P}}}{\bar{\bar{T}}}T' \\ c_{32}P' \\ c_{42}P' + c_{43}Z' + c_{45}\dfrac{\bar{\bar{Z}}}{\bar{\bar{T}}}T' \\ c_{54}D' \end{pmatrix}, \tag{29}$$

where N', P', Z', and D' are the unknowns and T', I' are the environmental drivers.

3.3. Inverse method

An inverse method is used to solve for the model parameters, C_{11}, C_{12}, C_{15}, C_{16}, C_{22}, C_{23}, C_{25}, C_{32},

Table 1
Parameters of the nonlinear *NPZD* model where q_{10p} stands for the growth rate of phytoplankton at 10 °C, I_o is the optimum solar radiation, K_N is the half saturation constant for N uptake by P, m_p is the mortality rate of phytoplankton, q_{10z} is the predation rate of zooplankton at 10 °C, β is the assimilation efficiency of zooplankton, m_z is the mortality rate of zooplankton, K_p is the half saturation constant for P uptake by Z and γ is the decomposition rate of detritus

Symbol	q_{10p}	I_o	K_N	m_p	q_{10z}	β	m_z	K_p	γ
Case 0	2.0	100	0.5	0.05	1.0	0.4	0.15	0.8	0.02
Case 1	2.4	S	S	S	S	S	S	S	S
Case 2	1.8	S	S	S	S	S	S	S	S
Case 3	S	S	0.7	S	S	S	S	S	S
Case 4	S	S	0.3	S	S	S	S	S	S
Case 5	S	120	S	S	S	S	S	S	S
Case 6	S	80	S	S	S	S	S	S	S
Case 7	S	S	S	0.15	S	S	S	S	S
Case 8	S	S	S	0.02	S	S	S	S	S
Case 9	S	S	S	S	1.2	S	S	S	S
Case 10	S	S	S	S	0.8	S	S	S	S
Case 11	S	S	S	S	S	S	0.05	S	S
Case 12	S	S	S	S	S	S	0.20	S	S
Case 13	S	S	S	S	S	S	S	1.0	S
Case 14	S	S	S	S	S	S	S	0.5	S
Case 15	S	S	S	S	S	0.6	S	S	S
Case 16	S	S	S	S	S	0.2	S	S	S
Case 17	S	S	S	S	S	S	S	S	0.03
Case 18	S	S	S	S	S	S	S	S	0.01
Unit	D^{-1}	Einsteins	mmol Nm^{-3}	D^{-1}	D^{-1}	–	D^{-1}	mmol Nm^{-3}	D^{-1}

S stands for the value same as in Case 0.

C_{42}, C_{43}, C_{45}, and C_{54}. Eq. (29) can be converted to a set of equations with respect to the model parameters, as shown here

$$\begin{pmatrix} -N' & -P' & -\frac{\bar{\bar{N}}}{\bar{\bar{T}}}T' & -\frac{\bar{\bar{N}}}{\bar{\bar{I}}}I' & 0 & 0 & 0 & 0 & 0 & 0 & 0 & D' \\ N' & P' & \frac{\bar{\bar{N}}}{\bar{\bar{T}}}T' & \frac{\bar{\bar{N}}}{\bar{\bar{I}}}I' & -P' & -Z' & -\frac{\bar{\bar{P}}}{\bar{\bar{T}}}T' & -P' & 0 & 0 & 0 & 0 \\ 0 & 0 & 0 & 0 & P' & Z' & \frac{\bar{\bar{P}}}{\bar{\bar{T}}}T' & 0 & -P' & -Z' & -\frac{\bar{\bar{Z}}}{\bar{\bar{T}}}T' & 0 \\ 0 & 0 & 0 & 0 & 0 & 0 & 0 & P' & P' & Z' & \frac{\bar{\bar{Z}}}{\bar{\bar{T}}}T' & -D' \end{pmatrix} \times \begin{pmatrix} c_{11} \\ c_{12} \\ c_{15} \\ c_{16} \\ c_{22} \\ c_{23} \\ c_{25} \\ c_{32} \\ c_{42} \\ c_{43} \\ c_{45} \\ c_{54} \end{pmatrix} = \begin{pmatrix} N' \\ P' \\ Z' \\ D' \end{pmatrix}. \tag{30}$$

This set of equations has more unknowns than equations, thus it is under-determined; however, Eq. (30) can be applied to each year data is available. Once there are sufficient observations, this equation may become over-determined and yield a unique solution. We introduce $\boldsymbol{A}(n)$ and $\boldsymbol{b}(n)$ to stand for the matrix on the left hand side of Eq. (30) and the vector on the right hand side at year n, respectively, and $\boldsymbol{c}$ for the vector of unknowns.

A least-squares objective function can written as,

$$J = \sum_{n=1}^{N} (\boldsymbol{A}(n)c - \boldsymbol{b}(n))^2, \tag{31}$$

where the vector of model parameters, $\boldsymbol{c}$, can be determined through minimizing J.

3.4. Prediction

After $\boldsymbol{c}$ is determined, Eq. (29) may be regarded as an equation set with respect to unknowns N', P', Z', and D', as given by

$$\begin{pmatrix} 1+c_{11} & c_{12} & 0 & -c_{54} \\ -c_{11} & 1-c_{12}+c_{22}+c_{32} & c_{23} & 0 \\ 0 & -c_{22}+c_{42} & 1-c_{23}+c_{43} & 0 \\ 0 & -c_{32}-c_{42} & -c_{43} & 1+c_{54} \end{pmatrix} \begin{pmatrix} N\prime \\ P\prime \\ Z\prime \\ D\prime \end{pmatrix} = \begin{pmatrix} -c_{15}\dfrac{\bar{\bar{N}}}{\bar{\bar{T}}}T' - c_{16}\dfrac{\bar{\bar{N}}}{\bar{\bar{T}}}I' \\ \left(c_{15}\dfrac{\bar{\bar{N}}}{\bar{\bar{T}}} - c_{25}\dfrac{\bar{\bar{P}}}{\bar{\bar{T}}}\right)T' + c_{16}\dfrac{\bar{\bar{N}}}{\bar{\bar{I}}}I' \\ \left(c_{25}\dfrac{\bar{\bar{P}}}{\bar{\bar{T}}} - c_{45}\dfrac{\bar{\bar{Z}}}{\bar{\bar{T}}}\right)T' \\ c_{45}\dfrac{\bar{\bar{Z}}}{\bar{\bar{T}}}T' \end{pmatrix} \tag{32}$$

The vector on the right hand side represents environmental forces. The matrix on the left hand side consists of components of vector $\boldsymbol{c}$ and maps year-to-year variations in the environmental driving to year-to-year variations in the ecosystem.

3.5. Data generation

To remove problems associated with data gaps, errors in measurements, and mismatches between model variables and actual observations, we run the *NPZD* model mentioned above to generate data. The environmental drivers required for model simulation include water temperature and solar radiation just below the water surface. We assume the water depth is shallow and both temperature and light are even. We use Eq. (A.1) (Appendix A) to generate temperature and light. Both temperature and light include a long-term mean, a year-to-year variation and a seasonal variation. The temperature has a long-term variation with a period of 10 years in the first 40 years and the light is similarly driven with a period of 15 years. In the next 40 years, both temperature and light have far less year-to-year variation than in the first 40 years. The purpose is to generate different year-to-year variations. Data generated in the first 40 years will be used for parameter estimation in the first order approximation model, and the data collected then after will be used to test the predictive capability of the model.

The initial conditions for the *NPZD* model are 1.0, 0.5, 0.2, and 3.0 mmol N m^{-3} for N, P, Z, and D, respectively. A simple Euler difference scheme is used to integrate the model equations (Eq. (26)). The time step is 0.1 h, and the model runs for 80 years. Values of N, P, Z, D, T, and I are output 10 times per year to develop annual mean data set (Fig. 2).

3.6. Parameter estimation

The data set collected in the first 40 years is used to estimate the model parameter vector $\boldsymbol{c}$ in Eq. (30). As Eq. (30) is linear, the minimization of $\boldsymbol{J}$, Eq. (31), may be achieved through solving an overdetermined linear equation set under a least-squares constraint. The solution vector $\boldsymbol{c}$ is listed in Table 2 as Case 0.

In order to examine how well the first order model approximates the observed (simulated) system, we compare predicted annual mean biases $\boldsymbol{x}'$ to observed (simulated) annual mean biases as follows. We use $\boldsymbol{c}$ along with the observed values of $\boldsymbol{x}'$, $\bar{\bar{\boldsymbol{x}}}$, $\boldsymbol{e}'$, and $\bar{\bar{\boldsymbol{e}}}$ to estimate $\boldsymbol{x}'$ via Eq. (29). This may appear to be circular reasoning, but inspection of Eq. (30) (or 31) reveals an important aspect in estimating $\boldsymbol{c}$. Because $\boldsymbol{x}'$ appears on both sides of Eq. (30), the value of $\boldsymbol{c}$ that

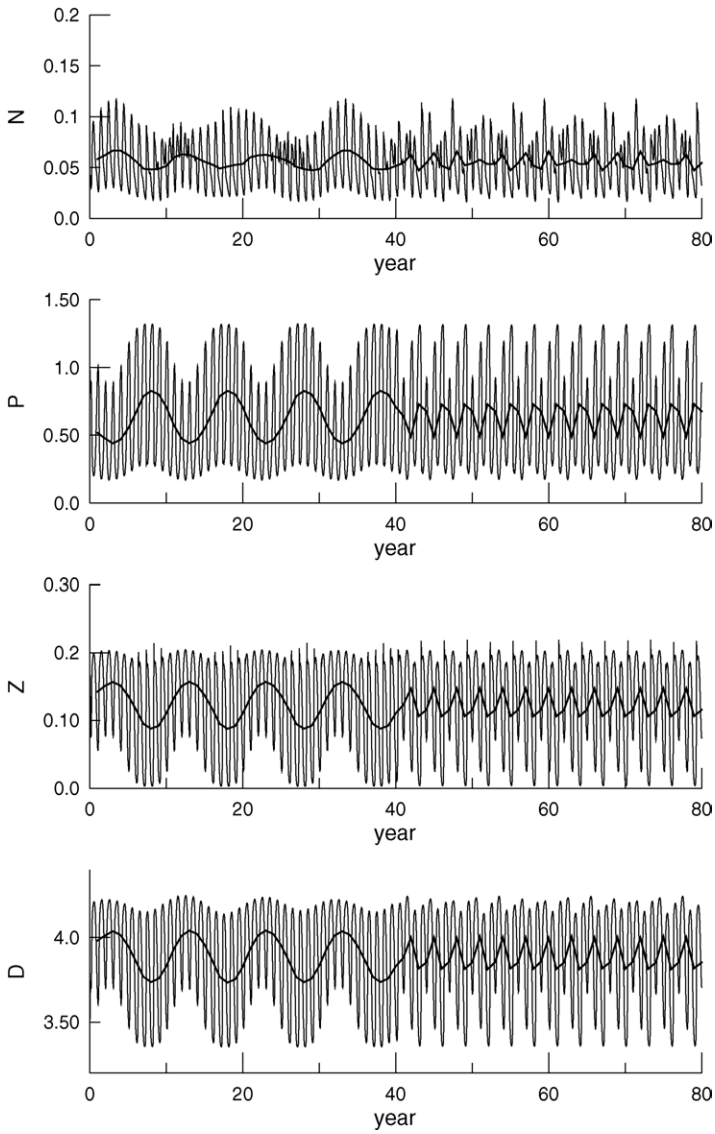

Fig. 2. Data generated with the *NPZD* model. The thin line stands for the seasonal dynamics and the thick line stands for annual means. *N*, *P*, *Z*, and *D* are concentrations of dissolve inorganic nutrient, phytoplankton, zooplankton and detritus, respectively. All variables are in units of mmol N m^{-3}.

minimizes Eq. (31) need not produce a model that conserves mass. Only when the first order model accurately represents the true system is mass conserved and the equality of Eq. (30) met. If mass conservation is significantly violated, then the predicted $\boldsymbol{x}'$ will not compare well to the observed $\boldsymbol{x}'$. Hence, by relaxing the mass conservation constraint in the minimization procedure, we obtain information on how well the first order model approximates the real system. In the simulated *NPZD* system, we see that the first order approximation, Eq. (29), is a good representation of the actual nonlinear system (Fig. 3). If the model fit to observations were poor, it would be necessary to reformulate the first order model, Eq. (29), using differ-

Table 2
Parameters of the first order approximation model and prediction precisions, where C_{11}, C_{12}, C_{13}, C_{14}, C_{21}, C_{22}, C_{23}, C_{31}, C_{41}, C_{42}, C_{43}, and C_{51}, are the first order approximation model parameters

Case	C_{11}	C_{12}	C_{13}	C_{14}	C_{21}	C_{22}	C_{23}	C_{31}	C_{41}	C_{42}	C_{43}	C_{51}	E_1 (%)	E_2 (%)
0	−0.39	0.29	0.005	0.003	−0.34	0.05	0.01	−0.34	−0.18	−0.01	−0.03	−0.33	76	73
1	−0.39	0.28	0.008	0.003	−0.35	0.04	0.01	−0.35	−0.18	−0.01	−0.03	−0.33	85	76
2	−0.39	0.29	0.007	0.003	−0.34	0.05	0.00	−0.34	−0.18	−0.01	−0.03	−0.34	59	61
3	−0.40	0.29	0.004	0.002	−0.34	0.06	0.00	−0.33	−0.18	0.00	−0.03	−0.34	60	62
4	−0.39	0.28	0.006	0.003	−0.35	0.03	0.01	−0.35	−0.19	−0.02	−0.03	−0.33	85	75
5	−0.39	0.29	0.000	0.003	−0.34	0.04	0.00	−0.35	−0.18	−0.01	−0.04	−0.34	75	69
6	−0.40	0.29	−0.01	0.003	−0.34	0.05	0.01	−0.34	−0.18	−0.01	−0.03	−0.34	65	65
7	−0.12	0.45	0.020	0.004	−0.48	0.03	0.05	−0.04	−0.04	0.03	0.10	−0.82	83	77
8	−0.61	0.28	0.010	0.003	−0.27	0.36	−0.08	−0.43	−0.24	−0.15	−0.06	−0.29	89	82
9	−0.40	0.31	−0.01	0.003	−0.33	0.06	−0.02	−0.34	−0.17	−0.00	−0.04	−0.34	89	82
10	−0.43	0.28	0.009	0.003	−0.35	0.11	−0.07	−0.34	−0.18	−0.08	0.11	−0.34	83	74
11	−0.30	0.44	−0.01	0.003	−0.34	0.16	−0.03	−0.17	−0.10	0.08	−0.03	−0.57	80	78
12	−0.51	0.27	0.006	0.004	−0.30	0.28	0.04	−0.37	−0.22	−0.19	0.12	−0.32	87	79
13	−0.41	0.28	0.020	0.003	−0.35	0.05	0.01	−0.35	−0.18	−0.02	0.01	−0.33	89	84
14	−0.45	0.35	0.009	0.009	−0.31	0.13	−0.06	−0.31	−0.16	0.03	−0.10	−0.38	85	80
15	−0.31	0.44	0.005	0.009	−0.33	0.18	−0.04	−0.18	−0.11	0.04	−0.03	−0.57	84	82
16	−0.44	0.27	0.004	0.003	−0.32	0.12	−0.02	−0.38	−0.20	−0.06	−0.01	−0.31	91	83
17	−0.41	0.30	0.009	0.003	−0.34	0.07	−0.01	−0.33	−0.18	−0.03	−0.01	−0.34	84	83
18	−0.37	0.28	0.008	0.003	−0.33	0.12	−0.05	−0.36	−0.20	−0.10	0.04	−0.33	86	77
19	−0.39	0.29	0.005	0.003	−0.34	0.05	0.01	−0.34	−0.18	−0.01	−0.03	−0.33	76	83
20	−0.39	0.29	0.005	0.003	−0.34	0.05	0.01	−0.34	−0.18	−0.01	−0.03	−0.33	76	52
21	−0.42	0.33	−0.09	0.01	−0.33	0.41	0.02	−0.16	−0.16	−0.20	0.57	−0.51	80	73

E_1, E_2 are the hindcast and forecast precisions. Case 0 is referred as the reference run, Cases 1–18 as the parameter sensitivity runs, Cases 19 and 20 as different environmental driving runs and Case 21 as the observation error run.

ent dependencies and perhaps different compartment connectivity.

3.7. Hindcast and forecast

The objective of the first order approximation model is to predict year-to-year variations of an ecosystem from the annual mean values of the environmental drivers, $\boldsymbol{e}'$, (T' and I' in this example), the long-term mean values $\bar{\bar{\boldsymbol{x}}}$ and $\bar{\bar{\boldsymbol{e}}}$ ($\bar{\bar{P}}$, $\bar{\bar{Z}}$, $\bar{\bar{T}}$, and $\bar{\bar{I}}$ here), and the vector $\boldsymbol{c}$ according to the prediction formulation (Eq. (32)).

For the simulated system, we run the prediction over 80 years, where the first 40 years may be considered as the hindcast period, and the next 40 years as the forecast period. The comparison of the predicted year-to-year variations against the data is shown in Fig. 4. The predicted variations match the data well in terms of both pattern and amplitude. To quantify model fit, we define the total mean prediction precision as,

$$\varepsilon_{1-40} = 100\left(1 - \frac{1}{4}\sum_{j=1}^{4}\frac{1/40\sum_{i=1}^{40}|\bar{x}_j^*(i) - \bar{\bar{x}}_j|}{\max_{i=1}^{40}|\bar{x}_j(i) - \bar{\bar{x}}_j|}\right),$$

$$\varepsilon_{41-80} = 100\left(1 - \frac{1}{4}\sum_{j=1}^{4}\frac{1/40\sum_{i=41}^{80}|\bar{x}_j^*(i) - \bar{\bar{x}}_j|}{\max_{i=1}^{40}|\bar{x}_j(i) - \bar{\bar{x}}_j|}\right), \quad (33)$$

where ε_{1-40} stands for the hindcast precision, ε_{41-80} for the forecast precision, and x_1^*, x_2^*, x_3^*, and x_4^* for N, P, Z, and D, respectively. For the model fit based on the first 40 years of data, ε_{1-40} and ε_{41-80} equal 76 and 73%, respectively (Table 2, Case 0). This error analysis indicates that the model fits the observations well, based on hindcast results, and that the model forecast does not degrade even when environmental drivers differ from those used to calibrate the model.

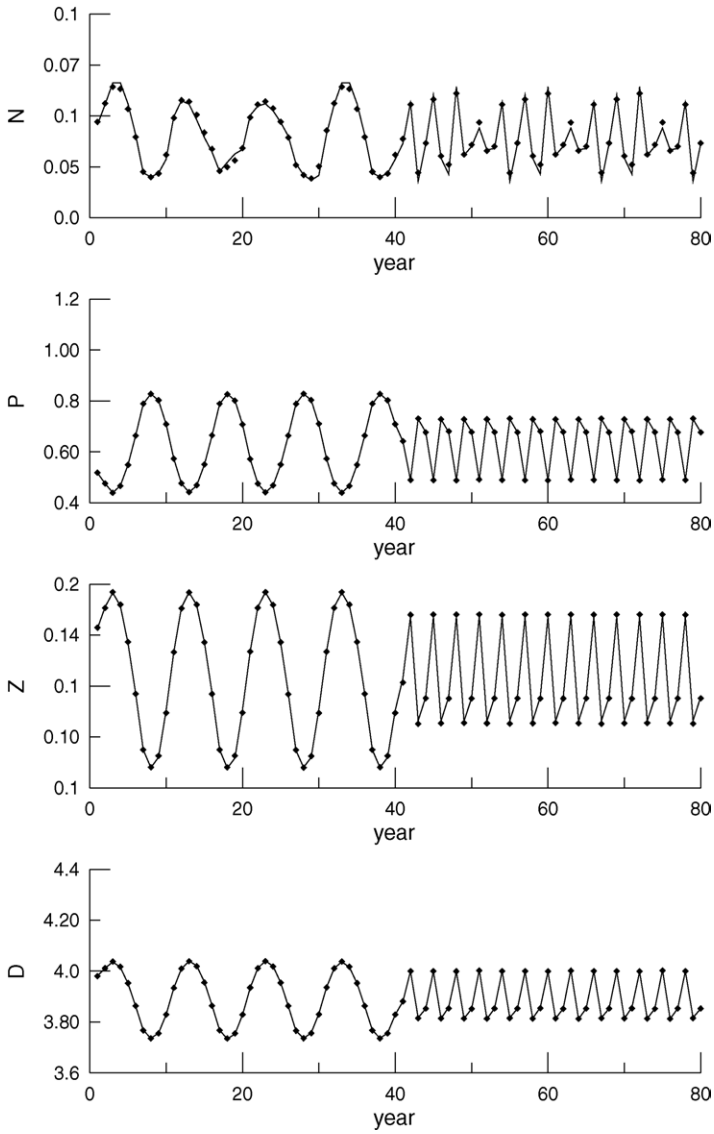

Fig. 3. Comparison of the first order approximation (solid line) with data (diamond) during following data assimilation via Eqs. (30) and (31). Note, because of the implicit nature of Eq. (30), mass need not be conserved. All variables are in units of mmol N m^{-3}.

4. Model analysis and discussion

4.1. Parameter sensitivity

The vector $\boldsymbol{c}$ contains the parameters of the first order approximation model, but the value of $\boldsymbol{c}$ depends on the parameters of the simulation, or true, model (Eq. (26), Table 1). Changes of the simulation model parameters represent different ecosystems that have similar structures and connections, but perhaps different species. We want to examine how the first order model responds, both in accuracy of fit and value of $\boldsymbol{c}$, to parameter changes in the simulated model, Eq. (26). To accomplish this, we changed one parameter value at a time and ran the NPZD model to regenerate a data set as we did in Case 0, then examined the fit statistics, Eq.

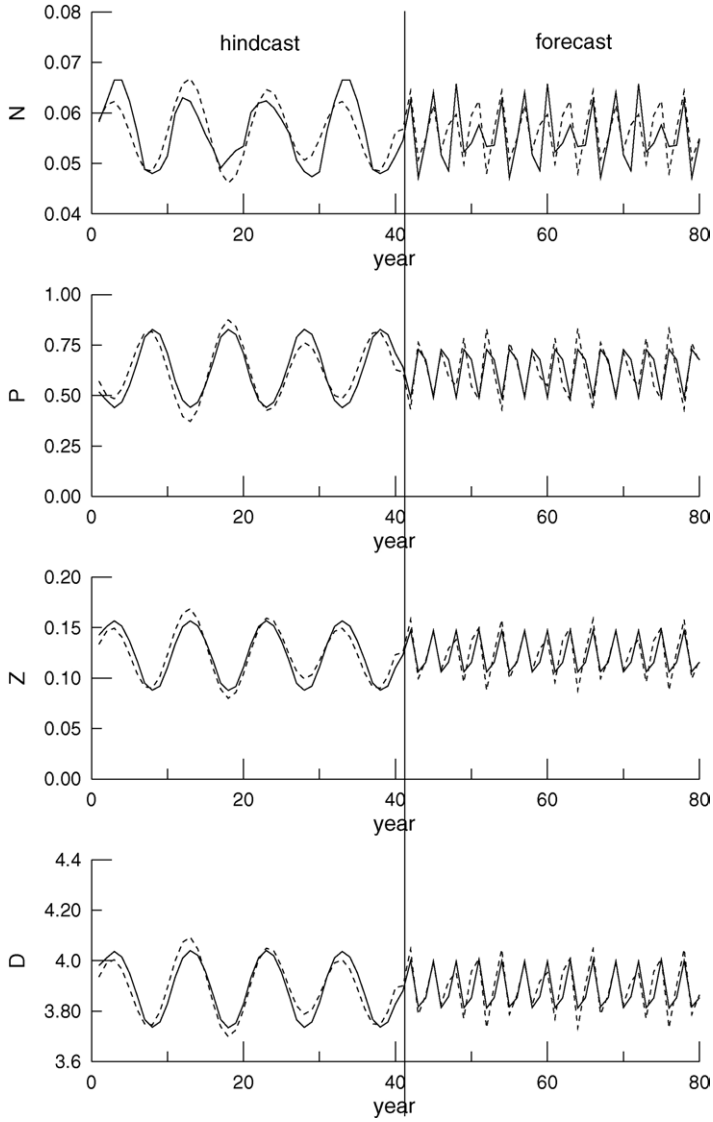

Fig. 4. Comparison of predicted year-to-year variations (dashed line) by the first order approximation model (Eq. (32), mass conserving) to data (solid line) generated with the nonlinear model (Eq. (26)). The nonlinear model is run under environmental drivers of Eq. (A.1) and with parameters listed in Table 1 as Case 0. All variables are in units of mmol N m^{-3}.

(33), and the new $\boldsymbol{c}$ values obtained from minimizing Eq. (31). Parameters in the simulation model were increased or decreased by as much as 100% (Table 1), but we decreased the magnitude of the parameter perturbation if the perturbation resulted in an unstable simulation. For instance, when q_{10P} is increased from 2.0 to 4.0, the ecosystem collapses, which is not of interest for the sensitivity analysis.

The estimated $\boldsymbol{c}$ values and the prediction precisions for each perturbation (Table 1) are listed in Table 2 as Cases 1–18. In the first 19 cases (0–18), the prediction precisions are mostly higher than 70%, and the hindcast precision is slightly higher than the forecast precision. The high prediction precision indicates the first order approximation model accurately describes year-to-year variations of the ecosystem regardless of the param-

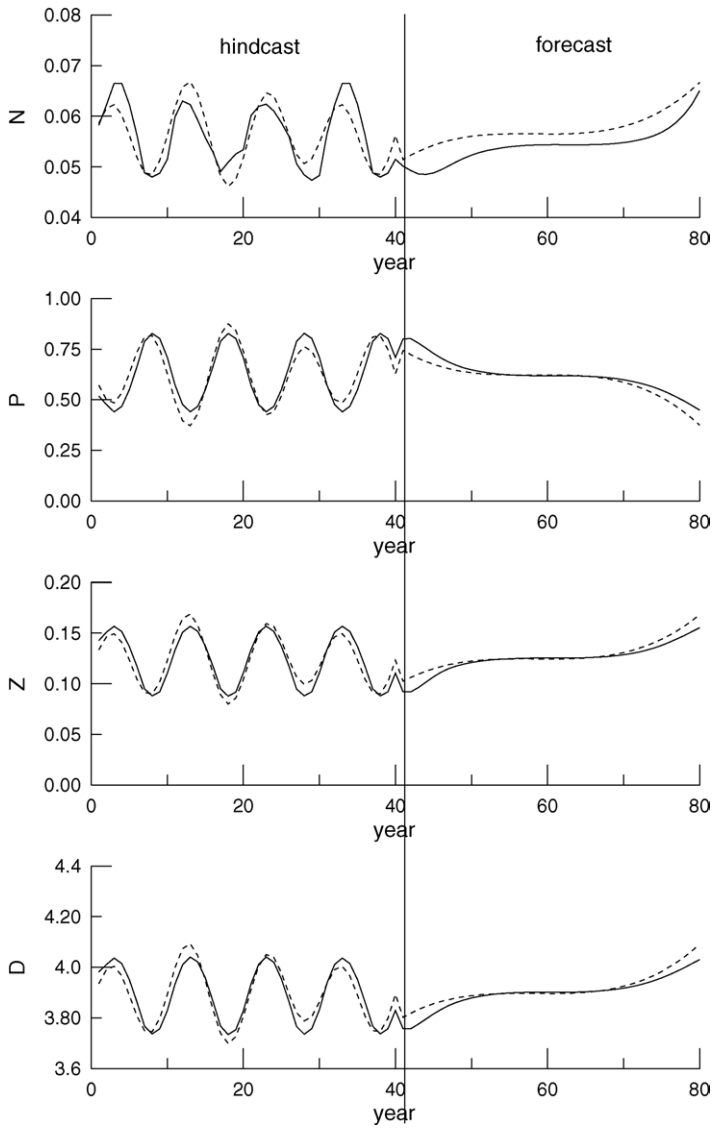

Fig. 5. Comparison of predicted year-to-year variations (dashed line) with the first order approximation model (Eq. (32)) to data (solid line) generated with the nonlinear model (Eq. (26)). The nonlinear model is run under environmental drivers of Eq. (A.2) and with parameters listed in Table 1 as Case 0. All variables are in units of mmol N m^{-3}.

eters used in the simulation model. Furthermore, the minimization, Eq. (31), is robust, since $\boldsymbol{c}$ does not vary significantly given large perturbations in the simulation model (Table 2), which is in contrast to parameter estimation in complex ecosystem models (Vallino, 2000; Fennel et al., 2001). The reasons for this robustness are a result of applying scaled (dimensionless) variables and use of a linear model.

4.2. Prediction capability against environmental driving

We examine two experiments to test the prediction capability of the first order model against changes in environmental driving. First, we change the form of the annual mean component of the environmental driving function from periodic to monotonically increas-

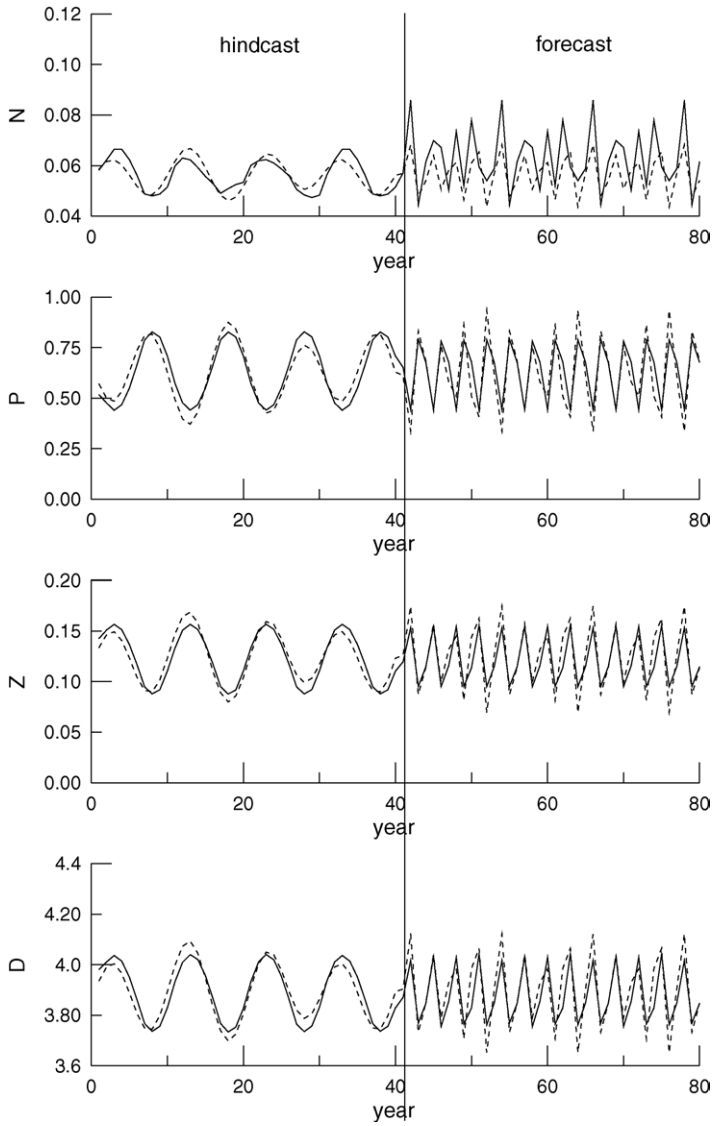

Fig. 6. Comparison of predicted year-to-year variations (dashed line) with the first order approximation model (Eq. (32) to data (solid line) generated with the nonlinear model (Eq. (26)). The nonlinear model is run under environmental drivers of Eq. (A.3) and with parameters listed in Table 1 as Case 0. All variables are in units of mmol N m^{-3}.

ing T or decreasing L function, which is more consistent with a global change scenario, given by Eq. (A.2) (Appendix A). For the first 40 years, we use the same environmental drivers as before, Eq. (A.1) (Appendix A), and use the same parameter vector, $\boldsymbol{c}$, as in Case 0, but refer to simulation as Case 19. Results show (Fig. 5, Table 2) that the first order model readily handles the change in driver form. For the second test, we increase the amplitude of year-to-year variations of environmental driving. We repeat the experiment of Case 0 again with the driving function for second 40 years, given by Eq. (A.3) (Appendix A). The results show some decrease in prediction precision (Table 2 as Case 20), but the first order approximation model still produces a very respectable forecast (Fig. 6).

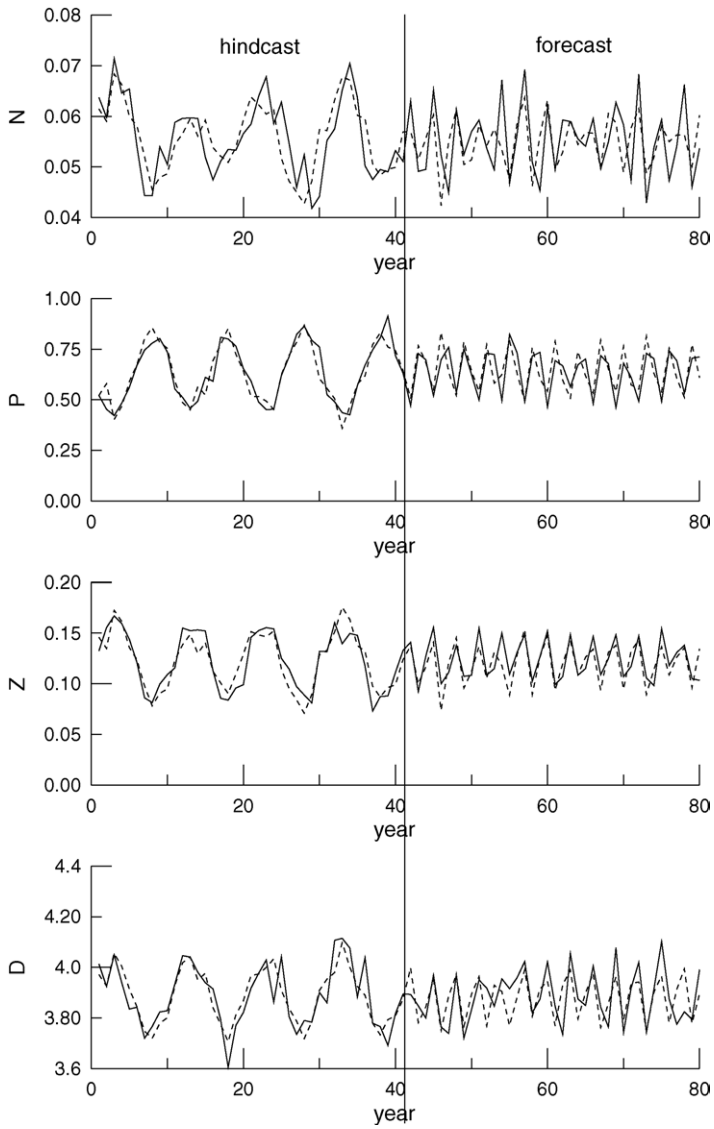

Fig. 7. Comparison of predicted year-to-year variations (dashed line) with the first order approximation model (Eq. (B.2)) to data (solid line), which is generated with the nonlinear model (Eq. (26)) and added a random error (Eq. (34)). The nonlinear model is run under environmental drivers of Eq. (A.1) and with parameters listed in Table 1 as Case 0. All variables are in units of mmol N m^{-3}.

We conducted several experiments similar to the two cases above, with similar results (data not presented). It appears that the form of driving function does not influence the prediction precision, but increasing the amplitude of the annual mean environmental driving variations does. If the environmental driver amplitude is higher than it is during the parameter calibration phase, then the prediction precision of the forecast is reduced.

4.3. Model performance with observation error

In the above simulations, we have employed noise-free data. In any real application, the model must perform accurately in the presence of observation errors. In order to test the model performance with data noise, we added a random error with amplitude of 30% of the long-term mean value to the generated data set. The

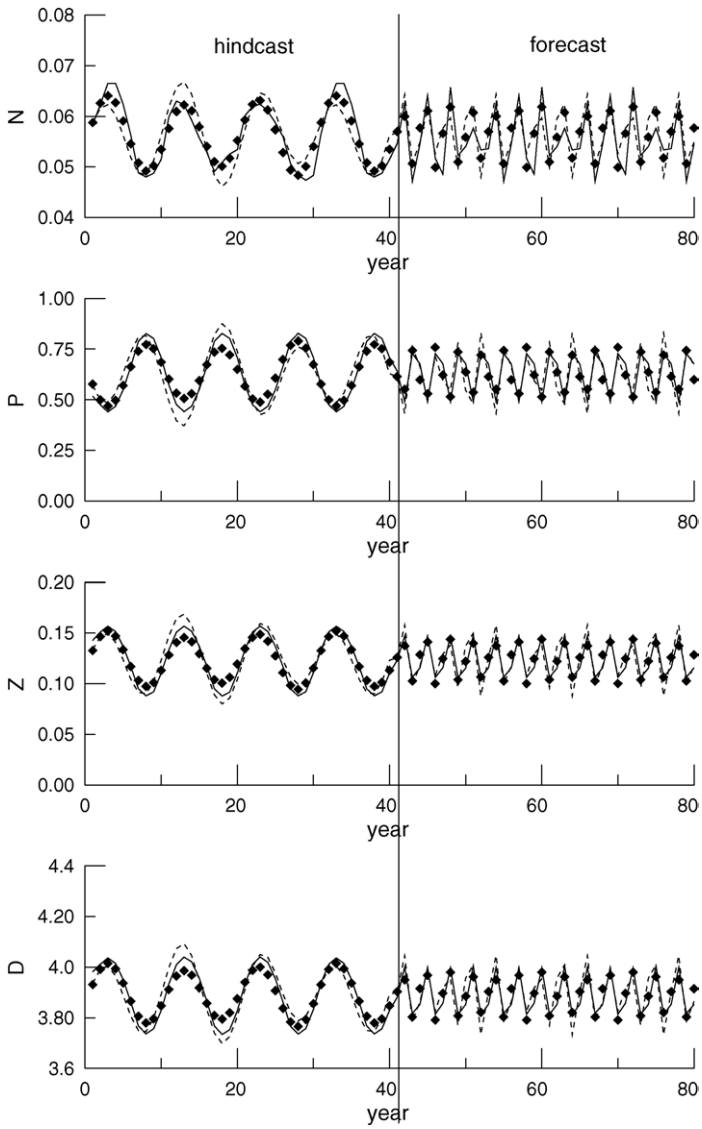

Fig. 8. Comparison of predicted year-to-year variations (dashed line) with the first order approximation model (Eq. (B.2)) to data (solid line) generated with the nonlinear model (Eq. (26)). The nonlinear model is run under environmental drivers of Eq. (A.1) and with parameters listed in Table 1 as Case 0. All variables are in units of mmol N m^{-3}.

generation of data noise is given by,

$$\begin{aligned}
\tilde{N}(i) &= N(i) + 30\% \cdot \bar{\bar{N}} \cdot \eta(i) \\
\tilde{P}(i) &= P(i) + 30\% \cdot \bar{\bar{P}} \cdot \eta(i) \\
\tilde{Z}(i) &= Z(i) + 30\% \cdot \bar{\bar{Z}} \cdot \eta(i) \\
\tilde{D}(i) &= D(i) + 10\% \cdot \bar{\bar{D}} \cdot \eta(i) \\
\tilde{T}(i) &= T(i) + 30\% \cdot \bar{\bar{T}} \cdot \eta(i) \\
\tilde{L}(i) &= L(i) + 30\% \cdot \bar{\bar{L}} \cdot \eta(i).
\end{aligned} \tag{34}$$

where $N(i)$, $P(i)$, $Z(i)$, $D(i)$, $T(i)$, and $L(i)$ stand for the values of N, P, Z, D, T, and L collected at ith time, respectively, and $\tilde{N}(i)$, $\tilde{P}(i)$, $\tilde{Z}(i)$, $\tilde{D}(i)$, $\tilde{T}(i)$, and $\tilde{L}(i)$ stand for the data added with noise. The function $\eta(i)$ generates a uniformly distributed random number η for each time i, where $\eta \in (0,1)$. Although prediction precision of both hindcast and forecast decrease (Table 2, Case 21), the prediction largely matches the

data (Fig. 7), which indicates the model is able to accurately assimilate noisy data. However, the addition of noise does cause a significant change in the first order model parameter vector, $\boldsymbol{c}$ (Table 2, Case 21 versus Case 0); it should be noted that the parameters are now fitted to the data + noise rather than the data alone.

4.4. First order approximation with less knowledge

The first order approximation *NPZD* model, Eq. (28), was developed according to the known flux expressions, Eq. (27), used to generate the simulated observations. Typically, such knowledge is unavailable; however, it is not necessary to have such detailed information to develop a useful first order model. To illustrate this robustness, we assume we only know the basic food web connectivity (Fig. 1) and employ basic reasoning to establish relationships between processes (i.e., fluxes) among the state and environmental drivers. We may get a more general first order approximation to year-to-year fluxes, similar to Eq. (28), with only the following differences,

$$f_3' = c_{32}N' + c_{33}P' + c_{35}\frac{\bar{\bar{P}}}{\bar{T}}T' + c_{36}\frac{\bar{\bar{P}}}{\bar{I}}I'$$
$$f_5' = c_{54}D' + c_{55}\frac{\bar{\bar{D}}}{\bar{T}}T'. \quad (35)$$

Similar to Eqs. (30) and (32), we can formulate an equation set (Eq. (A.1), Appendix A) about model parameters, c_{11}, c_{12}, c_{15}, c_{16}, c_{22}, c_{23}, c_{25}, c_{31}, c_{32}, c_{35}, c_{36}, c_{42}, c_{43}, c_{45}, c_{54}, and c_{55}, as well as a prediction equation (Eq. (A.2), Appendix A).

As the results indicate (Fig. 8), the change in model form does not decrease model performance, and the parameter values recovered are similar, where comparable, to those obtained in Case 0 (Table 3). In particular, parameters associated with flows that were not present in the original simulation model, Eq. (27), (namely, c_{31}, c_{35}, c_{36}, and c_{55} of Eq. (35)) have small or zero values (Table 3), which indicates the modeling approach is capable of discriminating between flow diagrams with differing degrees of connectivity. This example illustrates a possible approach to model development. It may be desirable to begin with a model that has high connectivity, then remove those connections that have small parameter coefficients following data assimilation. Of course, if the model lacks sufficient degrees of freedom, it will not be able to simulate the real system accurately. The technique demonstrated here can readably be extended to higher order approximations for ecosystems that exhibit highly nonlinear response to environmental drivers.

Table 3
Comparison of the two first order approximation models.Case 22 is the model run of the more general model (Eqs. (B.1) and (B.2)) and Case 0 is the model run of the model given by Eqs. (30) and (32)

	Case 22	Case 0
C_{11}	−0.64	−0.39
C_{12}	0.28	0.29
C_{13}	0.02	0.005
C_{14}	0.001	0.003
C_{21}	−0.34	−0.34
C_{22}	0.05	0.05
C_{23}	0.01	0.01
C_{31}	−0.09	None
C_{32}	−0.37	−0.34
C_{33}	0.001	None
C_{34}	−0.001	None
C_{41}	−0.18	−0.18
C_{42}	−0.01	−0.01
C_{43}	−0.04	−0.03
C_{51}	−0.34	−0.33
C_{52}	0.000	None
E_1 (%)	80	76
E_2 (%)	76	73

C_{11}, C_{12}, C_{13}, C_{14}, C_{21}, C_{22}, C_{23}, C_{31}, C_{32}, C_{33}, C_{34}, C_{41}, C_{42}, C_{43}, C_{51}, and C_{52}, are the first order approximation model parameters. E_1, E_2 are the hindcast and forecast precisions. 'none' means the model does not use this parameter.

5. Conclusion

We have developed a modeling approach that extends standard inverse modeling by using linearization, dimensional analysis, and time scale separation. This model is particularly targeted to forecasting long-term ecosystem dynamics that are largely governed by changes in environmental drivers. The model development is demonstrated with output from a simulated *NPZD* model. The approach is robust and captures year-to-year variations in the simulated ecosys-

tem. In case runs, this approach shows the following strengths: (1) the sensitivity of model parameters is relatively small, due to adoption of nondimensionalization; (2) the model tolerates a high signal-to-noise ratio in the data used to calibrate the model; (3) less knowledge on flux expressions for the food web is necessary in the first order approximation model. Case runs discovered, however, that the prediction precision is lower when the environmental driver amplitudes are higher than that under which the model is calibrated. The technique demonstrated here can be extended to higher order approximations if necessary.

Acknowledgement

This research was supported by NSF grant OPP-9911278.

Appendix A. Environmental drivers

Environmental drivers are expressed with notations θ standing for time (day), T for temperature (°C) and L for light (Einsteins) as followings,

$$\begin{aligned}
&\textbf{if } \theta \le 40 \times 365;\\
&\boldsymbol{T} = 10 + 8\sin\left(\frac{360\theta}{365} - 90\right) + 3\sin\left(\frac{360\theta}{10 \times 365}\right)\\
&\boldsymbol{L} = 100 + 80\sin\left(\frac{360\theta}{365} - 60\right) + 30\sin\left(\frac{360\theta}{15 \times 365}\right)\\
&\textbf{if } 40 \times 365 < \theta \le 80 \times 365;\\
&\boldsymbol{T} = 10 + 8\sin\left(\frac{360\theta}{365} - 90\right) + 3\sin\left(\frac{360\theta}{3 \times 365} - 180\right)\\
&\boldsymbol{L} = 100 + 80\sin\left(\frac{360\theta}{365} - 60\right) + 30\sin\left(\frac{360\theta}{4 \times 365} + 120\right),
\end{aligned} \tag{A.1}$$

$$\begin{aligned}
&\textbf{if } 40 \times 365 < \theta \le 80 \times 365;\\
&\boldsymbol{T} = 10 + 8\sin\left(\frac{360\theta}{365} - 90\right) + 3\left(\frac{\theta - 60 \times 365}{20 \times 365}\right)^3\\
&\boldsymbol{L} = 100 + 80\sin\left(\frac{360\theta}{365} - 60\right) - 30\left(\frac{\theta - 60 \times 365}{20 \times 365}\right)^2,
\end{aligned} \tag{A.2}$$

$$\begin{aligned}
&\textbf{if } 40 \times 365 < \theta \le 80 \times 365;\\
&\boldsymbol{T} = 10 + 8\sin\left(\frac{360\theta}{365} - 90\right) + 4.5\sin\left(\frac{360\theta}{3 \times 365} - 180\right)\\
&\boldsymbol{L} = 100 + 80\sin\left(\frac{360\theta}{365} - 60\right) + 45\sin\left(\frac{360\theta}{4 \times 365} + 120\right)
\end{aligned}. \tag{A.3}$$

Appendix B. A more general first order approximation model

The equation governing the parameters of the first order approximation,

$$\begin{pmatrix}
-N' & -P' & -\frac{\bar{\bar{N}}}{\bar{\bar{T}}}T' & -\frac{\bar{\bar{N}}}{\bar{\bar{I}}}I' & 0 & 0 & 0 & 0 & 0 & 0 & 0 & 0 & 0 & 0 & D' & \frac{\bar{\bar{D}}}{\bar{\bar{T}}}T' \\
N' & P' & \frac{\bar{\bar{N}}}{\bar{\bar{T}}}T' & \frac{\bar{\bar{N}}}{\bar{\bar{I}}}I' & -P' & -Z' & -\frac{\bar{\bar{P}}}{\bar{\bar{T}}}T' & -N' & -P' & -\frac{\bar{\bar{P}}}{\bar{\bar{T}}}T' & -\frac{\bar{\bar{P}}}{\bar{\bar{I}}}I' & 0 & 0 & 0 & 0 & \\
0 & 0 & 0 & 0 & P' & Z' & \frac{\bar{\bar{P}}}{\bar{\bar{T}}}T' & 0 & 0 & 0 & 0 & -P' & -Z' & \frac{\bar{\bar{Z}}}{\bar{\bar{T}}}T' & 0 & \\
0 & 0 & 0 & 0 & 0 & 0 & 0 & N' & P' & \frac{\bar{\bar{P}}}{\bar{\bar{T}}}T' & \frac{\bar{\bar{P}}}{\bar{\bar{I}}}I' & P' & Z' & \frac{\bar{\bar{Z}}}{\bar{\bar{T}}}T' & -D' & -\frac{\bar{\bar{D}}}{\bar{\bar{T}}}T'
\end{pmatrix}$$

$$\cdot \begin{pmatrix}
C_{11} \\ C_{12} \\ C_{15} \\ C_{16} \\ C_{22} \\ C_{23} \\ C_{25} \\ C_{31} \\ C_{32} \\ C_{35} \\ C_{36} \\ C_{42} \\ C_{43} \\ C_{45} \\ C_{54} \\ C_{55}
\end{pmatrix} = \begin{pmatrix} N' \\ P' \\ Z' \\ D' \end{pmatrix} \tag{B.1}$$

The first order approximation prediction equation with unknowns N', P', Z', and D',

$$\begin{pmatrix}
1 + c_{11} & c_{12} & 0 & -c_{54} \\
-c_{11} + c_{31} & 1 - c_{12} + c_{22} + c_{32} & c_{23} & 0 \\
0 & -c_{22} + c_{42} & 1 - c_{23} + c_{43} & 0 \\
c_{31} & -c_{32} - c_{42} & -c_{43} & 1 + c_{54}
\end{pmatrix} \begin{pmatrix} N' \\ P' \\ Z' \\ D' \end{pmatrix}$$

$$= \begin{pmatrix}
\left(-c_{15}\frac{\bar{\bar{N}}}{\bar{\bar{T}}} + c_{55}\frac{\bar{\bar{D}}}{\bar{\bar{T}}}\right)T' - c_{16}\frac{\bar{\bar{N}}}{\bar{\bar{I}}}I' \\
\left(c_{15}\frac{\bar{\bar{N}}}{\bar{\bar{T}}} - c_{25}\frac{\bar{\bar{p}}}{\bar{\bar{T}}} - c_{35}\frac{\bar{\bar{p}}}{\bar{\bar{T}}}\right)T' + \left(c_{16}\frac{\bar{\bar{N}}}{\bar{\bar{I}}} - c_{36}\frac{\bar{\bar{p}}}{\bar{\bar{I}}}\right)I' \\
\left(c_{25}\frac{\bar{\bar{p}}}{\bar{\bar{T}}} - c_{45}\frac{\bar{\bar{Z}}}{\bar{\bar{T}}}\right)T' \\
\left(c_{35}\frac{\bar{\bar{p}}}{\bar{\bar{T}}} + c_{45}\frac{\bar{\bar{Z}}}{\bar{\bar{T}}} - c_{55}\frac{\bar{\bar{D}}}{\bar{\bar{T}}}\right)T' + c_{36}\frac{\bar{\bar{p}}}{\bar{\bar{I}}}I'
\end{pmatrix} \tag{B.2}$$

References

van den Berg, H.A., 1998. Propagation of permanent perturbations in food chains and food webs. Ecol. Modell. 107, 225–235.

Diffendorfer, J.E., Richard, P.M., Dalrymple, G.H., et al., 2001. Applying linear programming to estimate fluxes in ecosystem or food webs: an example from the herpetological assemblage of the freshwater everglades. Ecol. Modell. 144, 99–120.

Ebert, U., Arrayas, M., Temme, N., et al., 2001. Critical condition for phytoplankton blooms. Bull. Math. Biol. 63, 1095–1124.

Eppley, R.W., 1972. Temperature and phytoplankton growth in the sea. Fish. Bull. 70, 1063–1085.

Fennel, K., Losch, M., Schröter, J., et al., 2001. Testing a marine ecosystem model: sensitivity analysis and parameter optimization. J. Marine Syst. 28, 45–63.

Kooi, B.W., Poggiale, J.C., Auger, P., et al., 2002. Aggregation method in food chains with nutrient recycling. Ecol. Modell. 157, 69–86.

Kooi, B.W., Poggiale, J.C., Auger, P., et al., 1998. Aggregation methods in food chains. Math. Comput. Modell. 27, 109–120.

Köhler, P., Wirtz, K.W., 2002. Linear understanding of a huge aquatic ecosystem model using a group-collecting sensitivity analysis. Environ. Modell. Software 17, 613–625.

Lischke, H., Löffler, T.J., Fischlin, A., 1997. Calculating temperature dependence over long time periods: derivation of methods. Ecol. Modell. 98, 105–122.

Nilsson, C., Grelsson, G., 1995. The fragility of ecosystems: a review. J. Appl. Ecol. 32, 677–692.

Steel, J.H., 1962. Environmental control of photosynthesis in the sea. Limnol. Oceanogr. 7, 137–150.

Stephen, D.W., Dunbar, S.R., 1993. Dimensional analysis in behavioral ecology. Behav. Ecol. 4 (2), 172–183.

Vallino, J.J., 2000. Improving marine ecosystem models: use of data assimilation and mesocosm experiments. J. Marine Res. 58, 117–164.

Vézina, A.F., Platt, T., 1988. Food web dynamics in the ocean. I. Best-estimates of flow networks using inverse methods. Marine Ecol. Prog. Ser. 42, 269–287.

Wan, Z., Yuan, Y., Qiao, F., 2000a. Study on optimization of the parameters of marine ecosystem dynamics model for red tide. Oceanol. Limnol. Sinica 31 (2), 205–209.

Wan, Z., Yuan, Y., Qiao, F., 2000b. The application of a continuous medium dynamics model for ocean plankton ecosystem. Acta Oceanologica Sinica 20(App), 239–249.